Engineering Stable Pacemaking at Physiological rate in Virtual Ventricular Myocytes

WC Tong, AV Holden

Institute of Membrane and Systems Biology, University of Leeds, Leeds, UK

Abstract

We evaluate the down-regulation of the time independent inward rectifying current (I_{K1}) and insertion of the hyperpolarisation-activated funny current (I_{f}) as methods to genetically engineer pacemaking in ventricular cells. The membrane systems (i.e., ionic concentrations clamped) of the Luo-Rudy dynamic cell model (LRd00) and a human ventricular cell model (HVM) are analysed using continuation algorithms with the maximum conductance ($\bar{g}$) of I_{K1} and I_{f} as bifurcation parameters. Autorhythmicity can be induced in both virtual ventricular models, either via Hopf or homoclinic bifurcations, by (1) reducing $\bar{g}_{\mathrm{K1}}$, (2) insertion of $\bar{g}_{\mathrm{f}}$, or (3) a combination of both. In the $\bar{g}_{\mathrm{f}}$-$\bar{g}_{\mathrm{K1}}$ parameter space of LRd00 membrane, unstable pacemaking activities clustered along the Hopf bifurcation boundary and with $\bar{g}_{\mathrm{K1}} \approx 0\,\mathrm{mS\,\mu F^{-1}}$. However, stable pacemaking with physiological rates can be induced by a combination of I_{K1} down-regulation and insertion of I_{f}.

1. Introduction

Ventricular cells are normally excitable and non-autorhythmic. However, autorhythmic ventricular cells have been genetically engineered experimentally. Miake *et. al.* [1, 2] induced autorhythmicity in guinea pig ventricular cells by the expression of Kir2.1AAA, a negative dominant gene construct which produced non-functional Kir2.1 channels and reduced I_{K1}. Qu *et. al.* and Plotnikov *et. al.* show that over expression of HCN2 isoforms in canine left atrium [3] and left bundle-branch [4] can drive the heart rhythm upon vagal stimulation-induced sinus arrest. These studies show that biological pacemakers can be engineered in mammalian heart.

The change from excitability to autorhythmicity is a qualitative change in system behaviour, *i.e.*, a bifurcation. Excitable neural cells can undergo a Hopf bifurcation (*HB*) into autorhythmicity by a reduction in potassium conductance [5, 6]. Ventricular cells can become autorhythmic through a *HB* with a constant depolarising current as the bifurcation parameter [7]. A *HB* occurs when a stable equilibrium lose its stability into small amplitude oscillations with a defined frequency.

Down-regulation of $\bar{g}_{\mathrm{K1}}$ in virtual mammalian ventricular cells induced autorhythmicity *via* a homoclinic bifurcation [8, 9, 10], where oscillations occur suddenly with an infinite period. The extremely low pacing rate due to the homoclinic bifurcation is a generic property for virtual mammalian ventricular cells and is clinically undesirable for a functional pacemaker. Nevertheless, stable autorhythmic action potentials occur away from the bifurcation point with greatly reduced $\bar{g}_{\mathrm{K1}}$. A combination of I_{K1} down-regulation and insertion of I_{f} may provides more flexibility for engineering stable pacemaking in mammalian ventricular hearts [11].

Here we apply continuation algorithms [12, 13] to biophysical detailed mammalian ventricular cell models, with the maximum conductance ($\bar{g}$) of I_{K1} and I_{f} as bifurcation parameters, to evaluate the proposed methods of genetically engineered pacemaking in ventricular cells and identify regions of stable pacemaking at physiological rates in the $\bar{g}_{\mathrm{f}}$-$\bar{g}_{\mathrm{K1}}$ parameter space.

2. Methods

We considered the epicardial membrane systems of the Luo-Rudy dynamic ventricular cell model (LRd00) [14] and the human ventricular cell model (HVM) by ten Tusscher *et. al.* [15], with clamped intra- and extra-cellular ionic concentrations at the standard initial values. For a single cell,

$$C_{\mathrm{m}} \frac{dV}{dt} = -I_{\mathrm{ion}} \ , \qquad (1)$$

where V is the membrane potential (mV); I_{ion} is the sum of membrane currents through ion channels, pumps and exchangers ($\mu\mathrm{A\,cm^{-2}}$); C_{m} is the membrane specific capacitance ($\mu\mathrm{F\,cm^{-2}}$).

Numerical solutions, equilibria and periodic states are computed using the package XPPAUT and the AUTO library [12, 13], with the fourth-order Runge-Kutta integrator and a fixed time-step of $0.002\,\mathrm{ms}$. Periodic solutions in HVM that cannot be reached *via* AUTO are integrated numerically using forward Euler and a variable time step

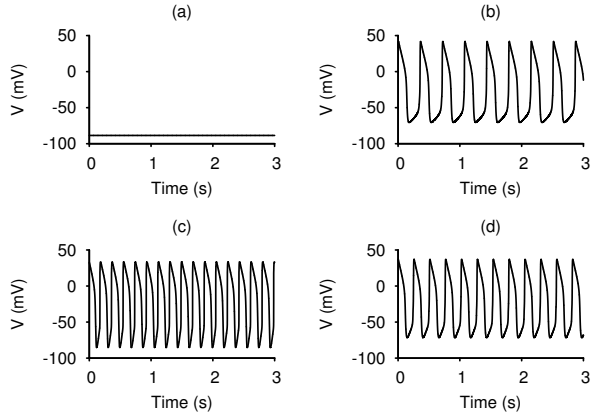

Figure 1. (*a*) $V(t)$ of a standard LRd00 remains at resting membrane potential ($\bar{g}_{\mathrm{K1}}$ = 0.75 mS $\mu\mathrm{F}^{-1}$, $\bar{g}_{\mathrm{f}}$ = 0 mS $\mu\mathrm{F}^{-1}$). (*b*) Reduction of $\bar{g}_{\mathrm{K1}}$ ($\bar{g}_{\mathrm{K1}}$ = 0 mS $\mu\mathrm{F}^{-1}$, $\bar{g}_{\mathrm{f}}$ = 0 mS $\mu\mathrm{F}^{-1}$), (*c*) insertion of $\bar{g}_{\mathrm{f}}$ ($\bar{g}_{\mathrm{K1}}$ = 0.75 mS $\mu\mathrm{F}^{-1}$, $\bar{g}_{\mathrm{f}}$ = 1.785 mS $\mu\mathrm{F}^{-1}$) and (*d*) a combination of both ($\bar{g}_{\mathrm{K1}}$ = 0.03339 mS $\mu\mathrm{F}^{-1}$, $\bar{g}_{\mathrm{f}}$ = 0.513336 mS $\mu\mathrm{F}^{-1}$) can induce pacemaker activities.

of $0.0005 - 0.4$ ms until an equilibrium or a periodic state is reached. The oscillation periods are defined as the time interval between successive maxima of *V*.

Down regulation of I_{K1} and insertion of I_{f} are modelled *via* their maximum conductances. I_{K1} is a time independent current that contributes to the maintenance of the resting membrane potential. For LRd00, physiological $\bar{g}_{\mathrm{K1}}$ = 0.75 mS $\mu\mathrm{F}^{-1}$; for HVM, physiological $\bar{g}_{\mathrm{K1}}$ = 5.405 mS $\mu\mathrm{F}^{-1}$. I_{f} is a voltage-gated pacemaking current not normally found in ventricular cells but it can be inserted in LRd00 and HVM with physiological $\bar{g}_{\mathrm{f}}$ = 0 mS $\mu\mathrm{F}^{-1}$. I_{f} is formulated as a Hodgkin-Huxley type voltage-gated current with a single activation variable and the equations are in [16]. It consists of a sodium and a potassium components with a conductance ratio of 0.3833:0.6167. We assumed this ratio is independent of $\bar{g}_{\mathrm{f}}$ and changes in $\bar{g}_{\mathrm{f}}$ does not affect the channel kinetics.

3. Results

Either down regulation of I_{K1} and insertion of I_{f} can induced pacemaking in ventricular cells (Figure 1). Pacemaking activities induced by complete block of I_{K1} are slow and have an elevated pacemaking potential. Insertion of I_{f} induced faster pacemaking activities closer to the normal resting membrane potential of ventricular cell. A combination of both induced activities with intermediate features.

The maximum and minimum *V* at different values of $\bar{g}_{\mathrm{K1}}$ and $\bar{g}_{\mathrm{f}}$, and their corresponding pacemaking periods are mapped onto the bifurcation diagram (Figure 2). Au-

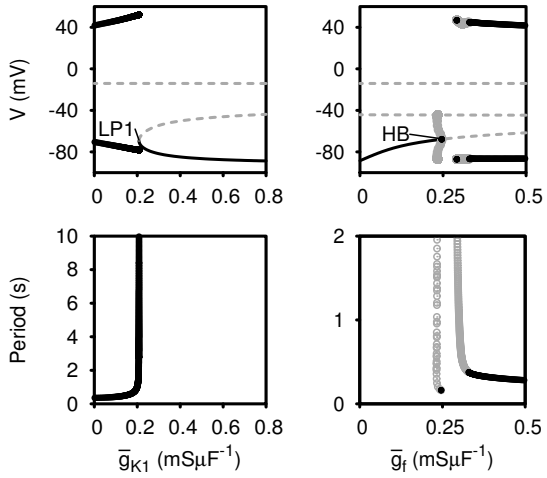

Figure 2. Bifurcation diagrams of the LRd00 membrane system for (*a*) $\bar{g}_{\mathrm{K1}}$ down-regulation and (*b*) $\bar{g}_{\mathrm{f}}$ insertion . Upper panels show the membrane potential (*V*) at which dV/dt = 0. Lower panels show the corresponding periods. Stable (*solid line*) and unstable (*dotted line*) equilibria, stable (*black solid circles*) and unstable (*grey empty circles*) periodic solutions, limit points (*LP*) and Hopf bifurcation (*HB*) are tracked using AUTO. A homoclinic bifurcation occur *LP1* at $\bar{g}_{\mathrm{K1}} \approx 0.225$ mS $\mu\mathrm{F}^{-1}$. A subcritical *HB* is found at $\bar{g}_{\mathrm{f}} \approx 0.25$ mS $\mu\mathrm{F}^{-1}$ and a limit point at $\bar{g}_{\mathrm{f}} \approx 2.007$ mS $\mu\mathrm{F}^{-1}$ (*LP2*, not shown). Physiological $\bar{g}_{\mathrm{K1}}$ = 0.75 mS $\mu\mathrm{F}^{-1}$; $\bar{g}_{\mathrm{f}}$ = 0 mS $\mu\mathrm{F}^{-1}$.

torhythmicity can be induced either *via* Hopf or homoclinic bifurcations. In either case, (reducing $\bar{g}_{\mathrm{K1}}$ or increasing $\bar{g}_{\mathrm{f}}$) resting membrane potential depolarised as the parameter moves away from the initial equilibrium ($\bar{g}_{\mathrm{K1}}$ = 0.75 mS $\mu\mathrm{F}^{-1}$ and $\bar{g}_{\mathrm{f}}$ = 0 mS $\mu\mathrm{F}^{-1}$). As $\bar{g}_{\mathrm{K1}} \approx 0.225$ mS $\mu\mathrm{F}^{-1}$ (≈ 70 % reduction), autorhythmic action potentials emerge *via* infinitely large (> 10 s) periods, *i.e.*, a homoclinic bifurcation (Figure 2, *LP1*). The rate increases as $\bar{g}_{\mathrm{K1}}$ decreases further (at $\bar{g}_{\mathrm{K1}}$ = 0, period ≈ 0.36 s). These are consistent with the experimental results [1, 2]. In contrast, autorhythmicity emerge *via* a subcritical *HB* at $\bar{g}_{\mathrm{f}} \approx 0.25$ mS $\mu\mathrm{F}^{-1}$ into unstable small-amplitude oscillations, *i.e.*, stable equilibrium and unstable periodic solutions coexist over a range of $0.23 < \bar{g}_{\mathrm{f}} < 0.25$ mS $\mu\mathrm{F}^{-1}$. Irregular pacemaking activities occured *HB* $< \bar{g}_{\mathrm{f}} < 0.329$ mS $\mu\mathrm{F}^{-1}$ and stable autorhythmic action potentials occurred at $\bar{g}_{\mathrm{f}} > 0.329$ mS $\mu\mathrm{F}^{-1}$, with period ≈ 0.377 s. The period decreases as $\bar{g}_{\mathrm{f}}$ increases (at $\bar{g}_{\mathrm{f}}$ = 1.785 mS $\mu\mathrm{F}^{-1}$, period ≈ 0.187 s).

For HVM, autorhythmicity are also induced either *via* Hopf or homoclinic bifurcations (Figure 3). Autorhythmic action potentials of large periods (> 10 s) emerge as $\bar{g}_{\mathrm{K1}} \approx 0.27$ mS $\mu\mathrm{F}^{-1}$ (≈ 92 % decrease in I_{K1} [10]). The rate quickly increases as $\bar{g}_{\mathrm{K1}}$ decreases further (at $\bar{g}_{\mathrm{K1}}$ =

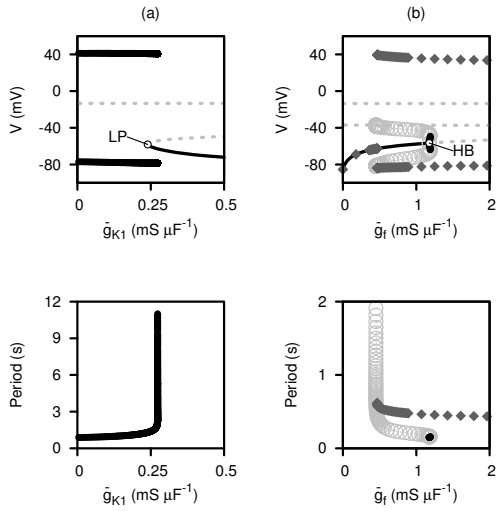

Figure 3. Bifurcation diagrams of the HVM membrane system for (*a*) $\bar{g}_{\mathrm{K1}}$ down-regulation and (*b*) $\bar{g}_{\mathrm{f}}$ insertion. Upper panels show the membrane potential (V) at which $dV/dt = 0$. Lower panels show the corresponding periods. Periodic solutions for $\bar{g}_{\mathrm{f}}$ insertion are computed with numerical integration (*diamonds*) and the corresponding periods are defined as the time period between successive maxima of V. Stable (*solid line*) and unstable (*dotted line*) equilibria, stable (*black solid circles*) and unstable (*grey empty circles*) periodic solutions, limit points (*LP*) and Hopf bifurcation (*HB*) are tracked using AUTO. A supercritical *HB* is found at $\bar{g}_{\mathrm{f}} \approx 1.17648\,\mathrm{mS\,\mu F^{-1}}$ and bistability occurs over a range of $0.450 < \bar{g}_{\mathrm{f}} < 1.19207\,\mathrm{mS\,\mu F^{-1}}$. Physiological $\bar{g}_{\mathrm{K1}} = 5.405\,\mathrm{mS\,\mu F^{-1}}$; $\bar{g}_{\mathrm{f}} = 0\,\mathrm{mS\,\mu F^{-1}}$.

$0\,\mathrm{mS\,\mu F^{-1}}$, period ≈ 1.136 s) suggest a homoclinic bifurcation. Insertion of I_{f} induced pacemaking activities *via* a supercritical *HB* at $\bar{g}_{\mathrm{f}} \approx 1.17648\,\mathrm{mS\,\mu F^{-1}}$, with stable small-amplitude oscillations ($-63 < V < -49$ mV, period range from $0.148 - 0.157$ s), over a narrow range of $1.17648 < \bar{g}_{\mathrm{f}} < 1.19207\,\mathrm{mS\,\mu F^{-1}}$. Numerical integration results show that stable autorhythmic action potentials occur before the *HB*, at $\bar{g}_{\mathrm{f}} \approx 0.450\,\mathrm{mS\,\mu F^{-1}}$ with period ≈ 0.620 s. The period decreases slowly as $\bar{g}_{\mathrm{f}}$ increases (at $\bar{g}_{\mathrm{f}} = 1.785\,\mathrm{mS\,\mu F^{-1}}$, period ≈ 0.438 s). Therefore, two bistability regions exist: (I) between a stable equilibrium and a stable oscillatory state within $0.450\,\mathrm{mS\,\mu F^{-1}} < \bar{g}_{\mathrm{f}} <$ *HB*, and (II) between two stable oscillatory states of different amplitude within *HB* $< \bar{g}_{\mathrm{f}} < 1.19207\,\mathrm{mS\,\mu F^{-1}}$. These are confirmed by numerical integration starting with different initial conditions.

Pacemaking activities induced by combining both methods show different pacemaking rates and stability in the $\bar{g}_{\mathrm{f}}$-$\bar{g}_{\mathrm{K1}}$ parameter space of LRd00 membrane (Figure 4). Majority of the slow (*i.e.*, with large periods) and unstable pacemaking activities are along the *HB* boundary and with $\bar{g}_{\mathrm{K1}} \approx 0\,\mathrm{mS\,\mu F^{-1}}$, and stable pacemaking activities at physiological ranges ($0.158 - 0.260$ s for guinea-pig) can be induced away from these unstable regions.

4. Discussion and conclusions

Continuation algorithms applied in the multi-parameter bifurcation spaces of virtual cardiac tissues offer a tool for engineering the dynamical behaviours of the heart. Autorhythmicity can be induced in virtual mammalian ventricular cells, either *via* a Hopf bifurcation or a homoclinic bifurcation, by (1) reducing $\bar{g}_{\mathrm{K1}}$, (2) insertion of $\bar{g}_{\mathrm{f}}$, or (3) a combination of both. In the parameter space of $\bar{g}_{\mathrm{K1}}$ and $\bar{g}_{\mathrm{f}}$, unstable oscillatory states clustered along the Hopf bifurcation boundary, or with $\bar{g}_{\mathrm{K1}} \approx 0\,\mathrm{mS\,\mu F^{-1}}$. However, a range of stable physiological oscillation periods from $0.2 - 0.4$ ms can be induced by a combination of I_{K1} down-regulation and insertion of I_{f}.

We have considered an idealised and simplified situation where ionic concentrations are kept constant. However, numerical integration of the full systems with either I_{K1} down-regulation or I_{f} insertion alone showed pacemaking may be transient particularly near the bifurcation points, due to the accumulation of $[\mathrm{Na}^+]_{\mathrm{i}}$ and $[\mathrm{Ca}^{2+}]_{\mathrm{i}}$ (results not shown). Complex behaviour including bursting and termination of pacing are observed and are further investigated with human models elsewhere [10, 17].

Changes in a single conductance designed to induce pacemaking may disturb the balance of intracellular ionic concentrations. Changing two conductances to genetically engineer pacemaking in ventricular cells may be beneficial in maintaining cell homeostasis during autorhythmicity. Isolated cells are integrated systems, and changes in a single conductance designed to produce pacemaking require compensatory changes in other ion transport and sequestration processes to maintain cell homeostasis.

Acknowledgements

This work was supported by the European Union through the Network of Excellence BioSim, Contract No. LHSB-CT-2004-005137. WCT is supported by a British Heart Foundation research studentship (FS/03/075/15914).

References

[1] Miake J, Marban E, Nuss HB. Biological pacemaker created by gene transfer. Nature 2002;419(6903):132–133.

[2] Miake J, Marban E, Nuss HB. Functional role of inward rectifier current in heart probed by Kir2.1 over expression and dominant-negative suppression. J Clin Invest 2003; 111(10):1529–1536.

[3] Qu J, Plotnikov AN, Danilo Jr P, Shlapakova I, Cohen IS, Robinson RB, Rosen MR. Expression and function of a

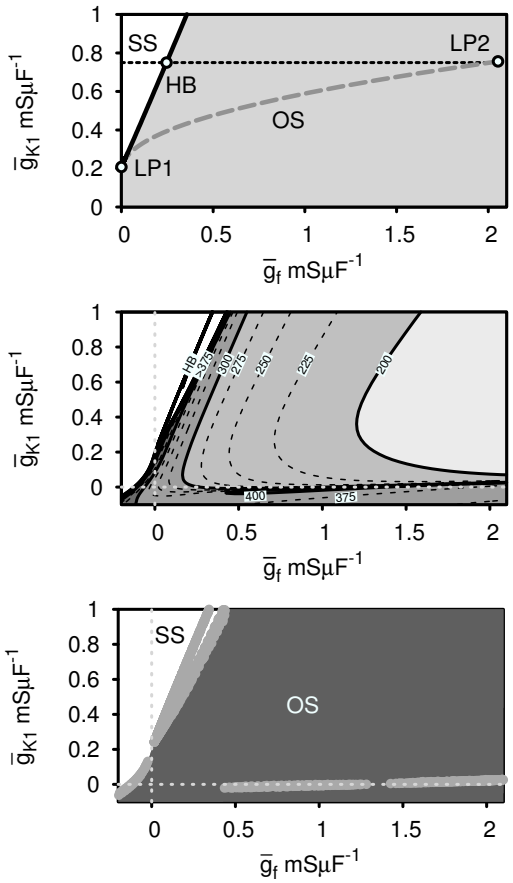

Figure 4. Two-parameter bifurcation diagrams for $\bar{g}_{\rm f}$ and $\bar{g}_{\rm K1}$ in LRd00 (*upper*), with the iso-periodic map (*middle*) and stability map (*bottom*) of the periodic states (*OS*). In the upper panel, *LP1*, *LP2* and *HB* are limit points and the Hopf bifurcation from Figure 2, and physiological $\bar{g}_{\rm K1} = 0.75\,{\rm mS\,\mu F^{-1}}$ (*dotted line*). *LP1* and *LP2* are connected by a fold (*dashed line*). A cusp point is found at a non-physical value (not shown). The *HB* (*solid line*) separates *OS* (*shaded area*) and the steady states (*SS*). Below $\bar{g}_{\rm f} \approx 0.00648\,{\rm mS\,\mu F^{-1}}$ and $\bar{g}_{\rm K1} \approx 0.223\,{\rm mS\,\mu F^{-1}}$, *OS* and *SS* are separated by the fold. Iso-lines of periods for every $100\,{\rm ms}$ (*solid line*) and every $25\,{\rm ms}$ (*dashed line*) are indicated in the middle panel. Majority of the *OS* are at periods within the physiological range except very close to the *HB* boundary where the periods shoots up to infinity. Iso-period $> 1\,{\rm ms}$ are not tracked. The stability map (*bottom*) shows most of the *OS* are stable (*dark grey*), unstable *OS* (*light gray*) are clustered along the *HB* boundary and with $\bar{g}_{\rm K1} \approx 0\,{\rm mS\,\mu F^{-1}}$.

biological pacemaker in canine heart. Circulation 2003; 107(8):1106–1109.

[4] Plotnikov AN, Sosunov EA, Qu J, Shlapakova IN, Anyukhovsky EP, Liu L, Janse MJ, Brink PR, Cohen IS, Robinson RB, Danilo Jr P, Rosen MR. Biological pacemaker implanted in canine left bundle branch provides ventricular escape rhythms that have physiologically acceptable rates. Circulation 2004;109(4):506–512.

[5] Holden AV, Yoda M. The effects of ionic channel density on neuronal function. J Theor Neurobiol 1981;1:61–81.

[6] Holden AV, Yoda M. Ionic channel density of excitable membranes can act a bifurcation parameter. Biol Cybern 1981;42(1):29–38.

[7] Chay TR, Lee YS. Phase resetting and bifurcation in the ventricular myocardium. Biophys J 1985;47(5):641–651.

[8] Benson AP, Holden AV, Clayton RH, Kharche S, Tong WC. Endogenous driving and synchronization in cardiac and uterine virtual tissues: bifurcations and local coupling. Phil Trans Roy Soc A 2006;364:1313–1327.

[9] Kurata Y, Hisatome I, Matsuda H, Shibamoto T. Dynamical mechanisms of pacemaker generation in IK1-down regulated human ventricular myocytes: insights from bifurcation analyses of a mathematical model. Biophys J 2005; 89(4):2865–2887.

[10] Tong WC, Holden AV. Induced pacemaker activity in virtual mammalian ventricular cells. LNCS 2005;3504:226–235.

[11] Tong WC, Holden AV. Bifurcation analysis of genetically engineered pacemaking in mammalian heart. J Biol Physic 2006;doi:10.1007/s10867-006-9004-1.

[12] Doedel EJ. AUTO: A program for the automatic bifurcation and analysis of autonomous systems. Cong Num 1981; 30:265–284.

[13] Ermentrout GB. XPPAUT. http://www.math.pitt.edu/∼bard/xpp/xpp.html.

[14] Faber GM, Rudy Y. Action potential and contractility changes in [Na(+)](i) overloaded cardiac myocytes: a simulation study. Biophys J 2000;78(5):2392–2404.

[15] ten Tusscher KH, Noble D, Noble PJ, Panfilov AV. A model for human ventricular tissue. Am J Physiol Heart Circ Physiol 2004;286(4):H1573–89.

[16] Azene EM, Xue T, Marban E, Tomaselli GF, Li RA. Non-equilibrium behavior of HCN channels: insights into the role of HCN channels in native and engineered pacemakers. Cardiovasc Res 2005;67(2):263–273.

[17] Zhang H, Tong WC, Garratt CJ, Holden AV. Stability of genetically engineered cardiac pacemaker: Role of intracellular Ca^{2+} handling. Comput Cardiol 2005;32:969–972.

Address for correspondence:

Wing Chiu Tong
Computational Biology Laboratory,
Institute of Membrane and Systems Biology,
University of Leeds,
Leeds LS2 9JT, UK
Email: cbs7wct@leeds.ac.uk